Numerical study of variability of technological parameters on remote coulomb scattering in nanowire MOSFETs

J. Dura[1,2], F. Triozon[1], D. Munteanu[2], S. Barraud[1], S. Martinie[1], J.L. Autran[2]

[1] CEA-LETI MINATEC, 17 rue des Martyrs, 38054 Grenoble, Cedex 9, France
[2] IM2NP-CNRS, UMR CNRS 6242, Bât. IRPHE, 49 rue Joliot Curie, BP 146, 13384 Marseille Cedex 13, France
(e-mail : julien.dura@im2np.fr, Phone: +33 4 38 78 65 32, Fax:+33 4 38 78 51 40)

***Abstract*-- In this paper, a theoretical study of electron mobility in nanowires MOSFETs is performed. The Kubo-Greenwood formula [1,2] is used and coupled to a self-consistent solution of the Schrödinger and Poisson equations for cylindrical gated silicon nanowires. Phonons and surface roughness scatterings are treated in accordance with literature [3-5]. This paper focuses on MOSFETs using high-k/metal gate stack. This configuration features a lot of trapped charges in the oxide which strongly affect the mobility especially at low inversion charge. Called remote coulomb scattering (RCS), it is modeled following Kubo-Greenwood approach including screening effect. The formalism of the Poisson solving considering a local charge in the oxide is given. Numerical results focus on the impact of technological parameters such as the amount of trapped charges in the oxide, the thickness of interfacial layer and the permittivity of the high-k dielectric on the RCS mobility. The idea is to support and to bring some orientations in the choice of materials and dimensions during the transistor technological process.**

Keywords – **Nanowire MOSFET, modeling, electronic mobility, screened RCS.**

I. INTRODUCTION

Due to the exploration of alternative solutions featuring high performances, nanoelectronic devices have evolved towards architectures allowing a much better electrostatics control of the device active region compared to conventional MOSFETs. GAA nanowires MOSFETs, regarding their particular shape, are one of the most promising architectures. This is due to the surface controlled by the surrounding gate which is significantly much higher than for planar devices. With this architecture (now considered as a realistic technology due to recent significant progress of technological processes [6,7]), it is possible to envisage ultra-scaled devices as required by the International Technology Roadmap for Semiconductor (ITRS, [8]). In order to assess potentialities of such ~~an~~ architecture, a deep understanding is required for the electronic transport. Although theoretical papers already investigated nanowire transport, it is hardly to make a link with technological process where defaults are generated. In this paper, we numerically investigated the electron mobility in nanowire including main limiting scattering mechanisms: phonon, surface roughness and ~~the~~ remote Coulomb scattering (RCS). This last mechanism is due to the non-perfect quality of process which traps charges in the gate oxide. So, in the following, we will particularly focus on the RCS and we will examine which parameters affect the mobility in order to support the technological process in the choice of dimensions or materials used in the transistor fabrication.

In the following, a cylindrical nanowire depicted in figure 1 is considered with a low-P-doped ($10^{15}cm^{-3}$) silicon channel delimited by highly N-doped source and drain regions. An interfacial *IL*/high-κ/metal gate stack is used with a metal (Al) gate work function equal to 4.3eV.

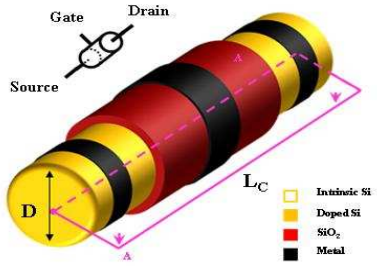

Fig. 1. Schematic of the GAA nanowire architecture and geometrical parameters definition.

II. KUBO-GREENWOOD INVESTIGATION FOR ELECTRON MOBILITY

A. The electronic band structure description

The electronic structure is obtained by computing a self-consistent Schrödinger-Poisson solver in cylindrical coordinates for a silicon nanowire oriented along the [001] axis. The 6 minima of the conduction band are described within the effective mass approximation. The 2 valleys along the [001] direction, named "longitudinal" valleys, have a confinement mass $m_t = 0.191m_e$ and a transport mass $m_l = 0.916m_e$, where m_e is the free electron mass. The 4 "transverse" valleys are anisotropic along the confinement directions. The cylindrical mass approximation is used here [5,9,10]: the confinement mass is $m_c = 2m_tm_l/(m_t+m_l)$ and the transport mass is m_t. This allows cylindrical symmetry to be used in the Schrödinger

This work is partially founded by the IBM-STMicroelectronics-CEA/LETI-MINATEC Development Alliance.

ISBN 978-0-615-71756-2

equation simplifying the system to one dimension. For thin nanowires (diameter < 5 nm), the effective mass approximation fails to describe accurately quantum confinement [10,11]. We modify the confinement masses given above in order to fit the energy levels given by a tight-binding calculation [12].

B. The Kubo-Greenwood theory

The mobility is computed in intrinsic cylindrical nanowires using the Kubo-Greenwood formula [1,2] based on the relaxation time approximation. Each interaction frequency is estimated using the Fermi golden rule based on the effective mass approximations corresponding to the probability to change from the initial state to the final one. The low-field electron mobility can be derived from the initial formula then modified to 1D transport [3] summing over the different valley α and subbands j:

$$\mu_{tot} = \frac{1}{n_{tot}} \sum_{\alpha j} n_{\alpha j} . \mu^{\alpha j} \tag{1}$$

where n_{tot} and $n_{\alpha j}$ are the total carrier concentration and the concentration in subband (α,j), respectively, and $\mu_{\alpha j}$ is the mobility of the subband expressed as:

$$\mu_{\alpha j} = \frac{2e}{kT . n_{\alpha j} . m_z^{\alpha}} \int_{E_{\alpha j}} g_{1D}^{\alpha j}(E) . (E - E_{\alpha j}) . \tau^{\alpha j}(E) . f(E) . (1 - f(E)) . dE \tag{2}$$

where m_z^{α} is the effective mass of valley α, $E_{\alpha j}$ is the energy level of the subband j of the valley α, $f(E)$ is the Fermi-Dirac statistics, $g_{1D}^{\alpha j}$ is the density-of-states of the subband j and $\tau^{\alpha j}$ is the total momentum relaxation time. The main scattering mechanisms pointed out by experimental investigations are considered: phonons *ph*, surface roughness *SR* and remote coulomb scattering *RCS*. The scattering by ionized dopants is not included because nanowires are considered intrinsic. The total momentum relaxation time is obtained by summing the scattering rates of all mechanisms:

$$\frac{1}{\tau_{tot}^{\alpha j}} = \frac{1}{\tau_{ph}^{\alpha j}} + \frac{1}{\tau_{SR}^{\alpha j}} + \frac{1}{\tau_{RCS}^{\alpha j}} \tag{3}$$

The scattering matrix elements for the phonons or surface roughness are widely spread in the literature using deformation potentials [3-5].

C. The Remote Coulomb Scattering (RCS)

The last mechanism, *RCS*, due to trapped charges in the high-k/metal gate stack is investigated by solving the Poisson equation considering a local charge in the oxide.
The matrix element of the RCS perturbation induced by a single coulomb center of charge Q at the position r_c is defined by (α,j is the initial state and α',j' is the final state):

$$V_{\alpha j, \alpha' j'}^{c} = \frac{Q}{L_c . \varepsilon_{Si}} . \int_0^{\infty} \varphi_{\alpha j} . \varphi_{\alpha' j'} . G_{lq}(r, r_c) . r . dr \tag{4}$$

where φ in the wave function, ε_{si} is the silicon permittivity, G is the Green function representing the dimensionless potential in the active region [10], l and q is the angular momentum and the wave vector difference between the initial and final state. The interest is to take into account the impact of the angular momentum on the mobility even if only the radial part of the wave function is used. The global matrix element of the system is easily obtained integrating the previous equation along all the trapped charge.

$$I_{\alpha j, \alpha' j'}^{c} = 2\pi L_c . \int_0^{\infty} n_c(r_c) . \left| V_{\alpha j, \alpha' j'}^{c} \right|^2 . r_c . dr_c \tag{5}$$

where $n_c(r_c)$ is the coulomb center density along the radius axis of the nanowire.

The momentum relaxation time is obtained by injecting this matrix element in the Fermi golden rule:

$$\frac{1}{\tau_{RCS}} = \frac{L_c . \sqrt{2m^{\alpha}}}{\hbar^2} \sum_{\alpha' j'} \delta_{\alpha \alpha'} I_{\alpha j, \alpha' j'}^{c} . \frac{\Theta(E - E_{\alpha j'})}{\sqrt{E - E_{\alpha j'}}} . \frac{1 + 2\beta[E - E_{\alpha j'}]}{\sqrt{E - E_{\alpha j'}}} \tag{6}$$

where β is the non-parabolic parameter.

The only term remaining to determine is $G_{lq}(r,r_c)$ which represents the normalized potential due to the charge localized in r_c with the retarded Green function satisfying the Poisson equation. Without screening effect, the Poisson equation in cylindrical coordinates is:

$$\left(\frac{\partial^2}{\partial r^2} + \frac{1}{r} . \frac{\partial}{\partial r} - q^2 - \frac{l^2}{r^2} \right) . G_{lq}(r, r_c) = \frac{\gamma}{r_c} . \delta(r - r_c) \tag{7}$$

with γ depends on the position of the charge (1 for a charge in the silicon film or $\varepsilon_{Si}/\varepsilon_{ox}$ for a charge in one of the gate oxide).

The Poisson equation in cylindrical coordinates has an explicit analytical solution thanks to the modified Bessel functions of the first (I) and second (K) order. The solution is inspired form [5] and the solution description for a high-κ/metal gate stack is given in [10]. (Notations r_i are defined on the figure 2)

$$G_{lq}(r, r_c) = \begin{cases} a I_l(qr) & 0 \prec r \prec rs \\ b I_l(qr) + c . K_l(qr) & rs \prec r \prec rox \\ d I_l(qr) + e . K_l(qr) & rox \prec r \prec rc \\ f I_l(qr) + h . K_l(qr) & rc \prec r \prec rm \end{cases} \tag{8}$$

where a, b, c, d, e, f and h are constants obtained with boundary conditions of the system.

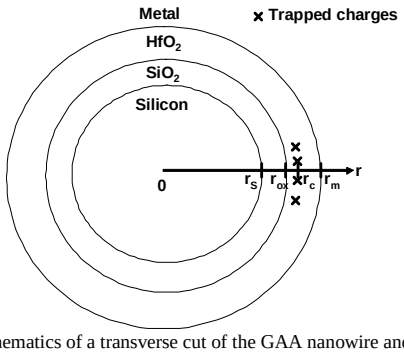

Fig. 2. Schematics of a transverse cut of the GAA nanowire and definition of notations for the different interfaces of the gate stack.

Then, screening effect due to the accumulated charge in the silicon film is considered using the Debye-Hückel approximation. In previous work, we highlighted an expression for the screened Green $\tilde{G}$ potential as a correction.

$$\tilde{G}_{lq}(r) = G_{lq}(r, r_c) + \frac{\frac{S}{\pi} G_{lq}(r, r_{max}) G_{lq}(r_{max}, r_c)}{1 + \frac{S}{\pi} G_{lq}(r_{max}, r_{max})} \quad (9)$$

where S is the screening parameter [10] and r_{max} is the maximum position of the wave function.

Main results are exposed in figure 2 with the Green function with respect to position along the nanowire radius and the scattering rate due to trapped charge in the gate oxide.

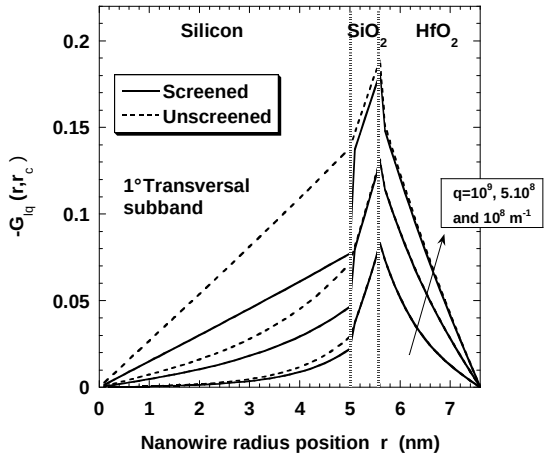

Fig. 2. Green function versus the position along the nanowire radius and for different wave vector and for the first transversal subband; Comparison between the screened and unscreened cases.

III.RESULTS – IMPACT OF TECHNOLOGICAL PARAMETRS

The objective of this part is to provide some results regarding the mobility dependence on parameter variations. As said in the introduction, MOSFETs are submitted to geometrical integration which leads to a reduction of dimensions as well as to the emergence of new materials. The interest is to highlight the impact of this integration on the electronic transport of carriers. Figure 3 shows the total mobility with respect to the electron density for different nanowire diameters. We can note that the electron mobility is strongly reduced for nanowire thinner than 10nm considering the same amount of trapped charge and the surface roughness.

In previous equations, we can note that several parameters such as dimensions or permittivity of oxides can significantly affect the RCS-limited mobility. In the previous result, all these parameters are taken in agreement with the literature: gate stack fixed on usual experimental observations and standard relative permittivity values for the silicon and hafnium oxides.

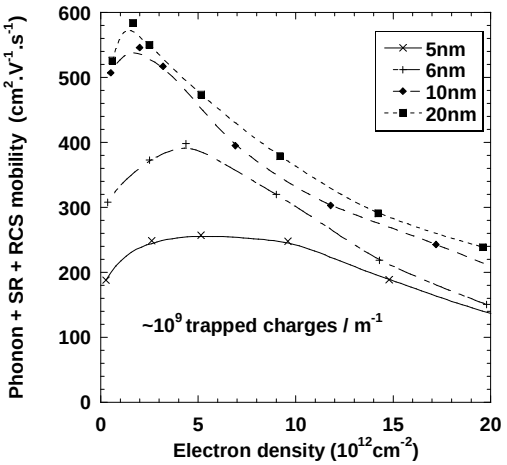

Fig. 3. Electron mobility versus the electron density for different nanowire diameters. t_{Sio2}=0.6nm; t_{Hfo2}=2nm; ε_{Sio2}=3.9; κ=18; N_{fix}=5.10^{12}cm^{-2}.

In the following, we will see what would happen with the mobility if technological process or materials are changed. Others parameters such as the amount of trapped charge depending on the process quality, the gate stack dimensions or the permittivity of dielectrics are considered using a 20nm-diameter nanowire. Figures 4 plots the total mobility depending on the electron density where the amount of trapped charges in the gate oxide varies. This is a real issue because we experimentally observe a large variability of this parameter (depending on the cross section of the nanowire for example [13]). As expected, increasing the amount of charge, the impact of the RCS is stronger and so the mobility decreases. The quality and the purity of the gate stack remains a great challenge in modern microelectronics.

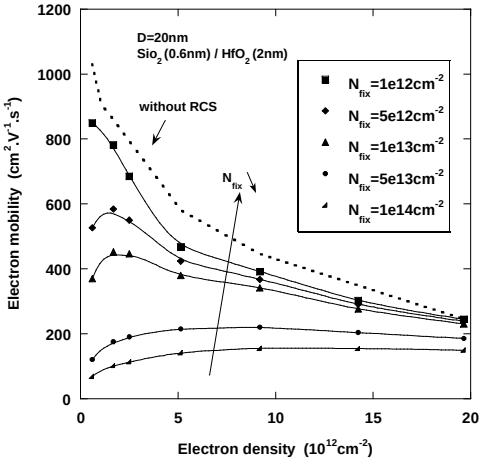

Fig. 4. Electron mobility versus the electron density for different amount of trapped charges in the double gate oxide. D=20nm; t_{Sio2}=0.6nm; t_{Hfo2}=2nm; ε_{Sio2}=3.9; κ=18.

Figures 5 and 6 plot the total electron mobility depending

on the electron density varying, respectively, the thickness of the *IL* (so the positions of trapped charges with respect to the silicon film) and the permittivity of the high-κ material. As expected, reducing the thickness of the SiO_2 layer leads trapped charges to come closer to the silicon film and so the electrostatic perturbation generated by these charges penetrates more in the silicon where carriers transport occurs. Consequently, the impact of the RCS is stronger and so the mobility decreases. Usually, we tend to reduce this layer in order to improve the electrostatic control of the device. But, with non-ideal dielectrics, the electronic transport is damaged.

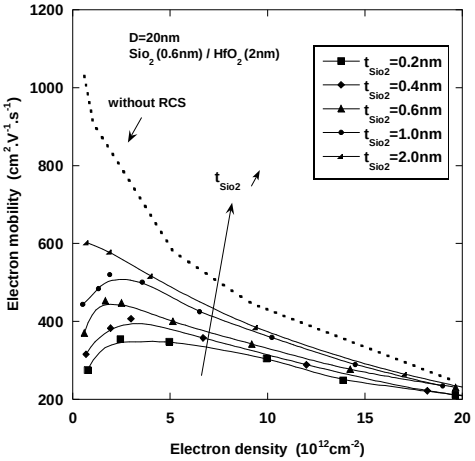

Fig. 5. Electron mobility versus the electron density for different interfacial silicon oxide layers in the high-κ/metal gate. D=20nm; t_{Hfo2}=2nm; ε_{Sio2}=3.9; κ=18, $N_{fix}=10^{13}cm^{-2}$.

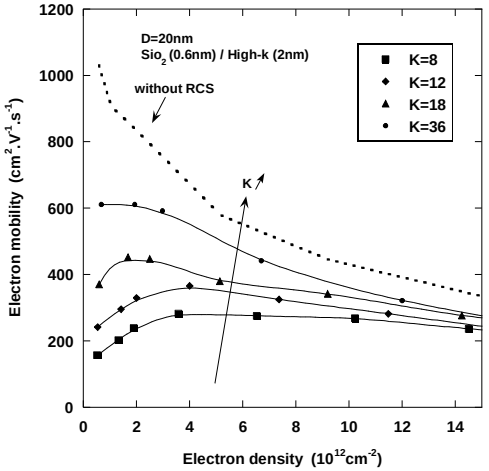

Fig. 6. Electron mobility versus the electron density for different high-κ layer permittivity. D=20nm; t_{Sio2}=0.6nm; t_{Hfo2}=2nm; ε_{Sio2}=3.9; $N_{fix}=10^{13}cm^{-2}$.

Regarding the permittivity, for higher values, the electrostatic envelop of trapped charges is less broaden in the silicon film and so the mobility increases especially at low-inversion charge. This can be a key observation in the choice of the high-κ materials. A compromise has to be found out between the quality of this oxide (to reduce N_{fix}) and its permittivity.

IV. CONCLUSION

A study of electronic transport in silicon nanowire is performed with the use of the Kubo-Greenwood formula including main limiting mechanisms observed in experiments (phonons, surface roughness and remote Coulomb scattering). This paper specially focused on this last phenomenon due to trapped charge in the gate oxide during the technology process. First, we have briefly developed the Fermi golden rule for the RCS scattering including screening effect based on a local charge at the *IL*/high-k interface. So, we could observe the impact of main parameters involved in the RCS limitation such as the nanowire diameter, the trapped charge density, the interfacial layer thickness and the high-k layer permittivity. The diameter has a great impact on the mobility for nanowire thinner than 10nm due essentially to phonon limitation. However, the trapped charge density, their position in the oxide and the oxide permittivity strongly affect the RCS component of the mobility. A compromise has to be found out between the permittivity of oxides and their quality in order to keep the electronic transport at an acceptable level.

REFERENCES

[1] R. Kubo, J. Phys. Soc. Jpn. 12, 570 (1957).
[2] D. A. Greenwood, Proc. Phys. Soc. London 71, 585 (1958).
[3] R. Kotlyar *et al*, Appl. Phys. Lett. 84, 5270 (2004).
[4] E. B. Ramayya *et al*, IEEE Trans. NanoTechnol. 6, 113 (2007).
[5] S. Jin *et al*, J. Appl. Phys. 102, 083715 (2007).
[6] K.H. Cho *et al*, *IEEE Electron Devices Letters*, vol. 28, no. 12, pp. 1129-1131 (2007).
[7] K. Tachi *et al.*, *IEDM Tech. Dig.*, pp.313-316 (2009).
[8] International Technology Roadmap for Semiconductors (2011).
[9] E. Gnani *et al*, IEEE Trans. Elec. Dev., vol. 54, 2243 (2007).
[10] J. Dura *et al*, J. Appl. Phys., vol. 111, 103710 (2012).
[11] A. Paussa *et al*, IEEE Trans. Elec. Dev ., vol. 57, 3239 (2010).
[12] J. Dura *et al*, Intech Open book, ISBN: 978-953-51-0239-7 (2012).
[13] M. Cassé *et al*, Appl. Phys. Lett., vol. 96, 123506 (2010).